

Picoliter Cell Lysate Assays in Microfluidic Droplet Compartments for Directed Enzyme Evolution

Balint Kintses,¹ Christopher Hein,¹ Mark F. Mohamed,¹ Martin Fischlechner,¹ Fabienne Courtois,¹ Céline Lainé,¹ and Florian Hollfelder^{1,*}

¹Department of Biochemistry, University of Cambridge, Cambridge CB2 1GA, UK

*Correspondence: fh111@cam.ac.uk

<http://dx.doi.org/10.1016/j.chembiol.2012.06.009>

SUMMARY

We demonstrate the utility of a microfluidic platform in which water-in-oil droplet compartments serve to miniaturize cell lysate assays by a million-fold for directed enzyme evolution. Screening hydrolytic activities of a promiscuous sulfatase demonstrates that this extreme miniaturization to the single-cell level does not come at a high price in signal quality. Moreover, the quantitative readout delivers a level of precision previously limited to screening methodologies with restricted throughput. The sorting of 3×10^7 monodisperse droplets per round of evolution leads to the enrichment of clones with improvements in activity (6-fold) and expression (6-fold). The detection of subtle differences in a larger number of screened clones provides the combination of high sensitivity and high-throughput needed to rescue a stalled directed evolution experiment and make it viable.

INTRODUCTION

The success of a directed evolution experiment strongly depends on the availability of efficient technologies for the exploration of the vastness of protein sequence space (Lin and Cornish, 2002; Turner, 2009). An ideal screening system for new enzyme catalysts would enable the identification of positive hits from a large number of variants, based on a precise assay readout. With advanced robotics, libraries of up to 10^6 clones can be screened (as colonies on agar plates or cell lysates in microwell plates), albeit at a high cost of time and resource (Agresti et al., 2010). These cost considerations and the general need for high-throughput make further miniaturization of assay volumes attractive. Screening of single cells by fluorescence-activated cell sorting (FACS) allows analysis of up to 10^8 clones but is only possible for specific selection schemes: The substrate has to diffuse into the cell and the fluorescent reaction product must be trapped inside or on the cell surface (Yang and Withers, 2009) to enable the colocalization of genotype (the enzyme-encoding gene) and phenotype (the reaction product) that is crucial for any directed evolution experiment.

To provide a general solution to the problem of how to retain the phenotype of enzyme reactions with the genotype, directed evolution assays have been compartmentalized into water-in-oil droplets (Schaerli and Hollfelder, 2009; Tawfik and Griffiths, 1998). Bulk emulsion droplets can be straightforwardly generated (albeit with ill-defined size) by dispersing water in oil and have been used for directed evolution in diverse selection formats (Leemhuis et al., 2005); e.g., for the evolution of polymerases (d'Abbadie et al., 2007; Loakes et al., 2009) or protein binders (Bertschinger et al., 2007). In these experimental setups, there is no need for quantitative measurement of the reaction product, as selection is based on self-amplification or affinity “panning.” In screening formats where the selectable trait is an optical readout, these droplets can be converted, by an additional emulsification step, to double emulsions (water-in-oil-in-water) and sorted by FACS. Although successful directed evolution of β -galactosidase (Mastrobattista et al., 2005) and serum paraoxonase (Aharoni et al., 2005; Gupta et al., 2011) has been demonstrated, this bulk emulsion protocol has been rarely used, despite its apparent convenience. Two emulsification events exacerbate droplet polydispersity: The variation in diameter is considerable and affects the quality of the optical measurement of concentration by a third power function. For evolution experiments where assay precision is crucial to take advantage of the typically small, incremental steps as directed evolution proceeds (Romero and Arnold, 2009), the inability to measure product concentrations accurately will be an impediment, leading to noisy data and possibly compromising the success of the screening effort.

To overcome the apparent limitations of bulk double emulsion droplets, monodisperse droplets can be generated in microfluidic devices (Schaerli and Hollfelder, 2009). Considerable technical effort has been devoted to incorporating in vitro evolution assays into microfluidic droplets for automated lab-on-a-chip systems for library screening and evolution (Kintses et al., 2010). It has been shown that the monodisperse droplets of microfluidic origin are suitable for quantitative assays (Huebner et al., 2008; Huebner et al., 2007). Compartmentalized single cells (Köster et al., 2008; Shim et al., 2009; Theberge et al., 2010) and in vitro expression from single genes (Courtois et al., 2008; Mazutis et al., 2009) provide “monoclonal droplets” as evolutionary units and set the scene for directed evolution in this format. Technical solutions to manipulate droplets to carry out such experiments have also been developed; e.g., droplet

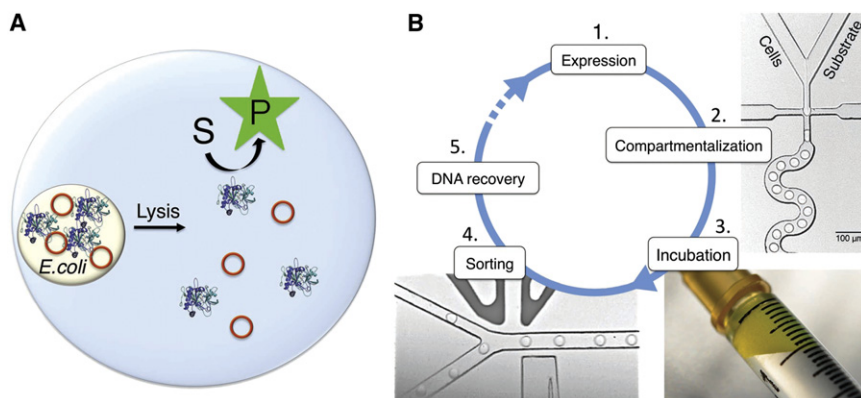


Figure 1. Schematic Directed Evolution Cycles by Lysate Screening in Droplets

(A) Library members are assayed in droplet compartments: An *E. coli* cell is lysed to expose intracellularly expressed enzyme (blue) to the co-compartmentalized substrate (S). The droplet compartment retains the resulting fluorescent product (P) with the enzyme-encoding plasmid DNA (red circles), constituting the genotype-phenotype linkage that enables directed evolution. (B) Workflow of the directed evolution experiment: (1) The protein of interest is expressed in *E. coli*; (2) single cells are compartmentalized together with substrate and cell lysis agents; (3) droplets are incubated to generate fluorescent product and (4) reinserted into a sorting device, where hits are detected by laser-induced fluorescence and steered into the upper channel by a variable

electric field (Movie S1); and (5) plasmid DNA from selected droplets is electroporated into *E. coli*. Repetition of such cycles increases the stringency of selection and enriches hits gradually to identify improved enzyme variants. See Figure S1 for the detailed designs of the microfluidic devices.

fusion (Mazutis et al., 2009; Niu et al., 2008), incubation (Frenz et al., 2009; Mazutis et al., 2009), or sorting (Baret et al., 2009; Fallah-Araghi et al., 2012) modules. However, the integration of multiple operations into a robust workflow of an evolution cycle has proven to be challenging (Kintses et al., 2010). Only one study is on record so far that has used microfluidic droplet sorting for evolution cycles, displaying the enzyme horseradish peroxidase on the surface of compartmentalized yeast cells (Agresti et al., 2010).

In this work, we extend this approach and present a microfluidic workflow that translates a frequently used screening procedure consisting of cytoplasmic protein expression, cell lysis, and assessment of reaction progress by fluorescence measurements to the picoliter droplet scale (Figure 1). To probe the utility of this workflow and to demonstrate the potential of droplet microfluidics for directed evolution, a fluorescent assay was set up for the detection of enzyme reactions in single-cell lysates, the precision of the optical readout was characterized and directed evolution performed on the arylsulfatase from *Pseudomonas aeruginosa* (PAS) (Boltes et al., 2001). PAS shows catalytically promiscuous activities (Babtie et al., 2009, 2010; Jonas and Hollfelder, 2009; Olguin et al., 2008; Mohamed and Hollfelder, 2012) that represent starting points for the evolution of new functions (O'Brien and Herschlag, 1999; Bornscheuer and Kazlauskas, 2004; Khersonsky and Tawfik, 2010). Our goal was to improve an existing promiscuous activity of PAS toward the nonnative substrate, phosphonate **3** (Figure 2). The successful selection of mutants with improved phosphonate hydrolase activity demonstrates that even rare events and small improvements in activity can be picked up in microfluidic droplet screening, combining high-throughput with high accuracy measurements.

RESULTS

Quality of the Assay Readout

Efficient evaluation of the clones during the directed evolution cycles depends on the precision of the assay readout. Therefore, prior to establishing a full evolution cycle, time courses of hydro-

lytic reactions with PAS were measured (in the device shown later in Figure 3A) to ensure that kinetic events are faithfully monitored in this miniaturized droplet-based assay format. PAS was expressed in *Escherichia coli* grown in liquid culture (Figure 1B, Step 1). Following overnight incubation (when cells are uniform in stationary growth phase), Poisson-distributed single cells are encapsulated in monodisperse droplets (Huebner et al., 2007, 2008; Shim et al., 2009) together with substrate and lysis agents (Steps 1 and 2 in Figure 1). The microfluidic set-up enables fast mixing upon droplet formation prior to cell lysis that removes the cellular barrier that would prevent polar and charged substrates to come in contact with an intracellularly produced enzyme. To obtain data on fast reactions (k_{cat}/K_M of PAS^{WT} with sulfate **2** (Figure 2) = $1.75 \times 10^5 \text{ M}^{-1}\text{s}^{-1}$) and short incubation times, droplets were driven through a long delay line directly after droplet formation, where individual droplets were analyzed by laser-induced fluorescence (Figure 3A). Figures 3B and 3C show the turnover of sulfate **2** by PAS^{WT} and its 8-fold slower mutant PAS^{H46Y,M72V}, representing a typical activity difference that needs to be distinguished in a round of directed evolution. The two populations are clearly separated, and the initial slopes of the progress curves reflect the activity difference of the two enzyme variants. The lag period prior to an increase of product fluorescence of PAS^{WT} can be ascribed to cell lysis that appears to occur in the first minute after mixing (Figures 3B and 3C), in a similar time interval as in microwells under identical conditions. This observation suggests an upper limit for the time-frame of reactions that can be followed: Time courses of reactions that give a significant product increase in a few minutes can be readily assayed. The accumulation of submicromolar concentrations of product **1** (Figure 2) can be detected for this substrate (for details, see Experimental Procedures). This amount of reaction product corresponds to only a few (~10) turnovers by PAS^{WT} contained in the cell lysate in the small droplet volume (20 pL). To obtain data for slow reactions, the time courses of the promiscuous activity of PAS^{WT} on phosphonate **3** ($k_{cat}/K_M = 2 \times 10^3 \text{ M}^{-1}\text{s}^{-1}$) were also followed (Figure 3D). Since no leakage of product **1** was observed in this format, the reaction mixture could be monitored for longer timescales. At each time

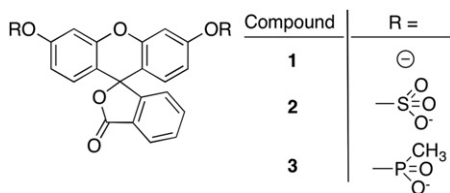


Figure 2. Hydrolytic Reactions of PAS

Fluorescein (**1**) is the reaction product of fluorescein disulfate (**2**) and bis(methylphosphonyl)-fluorescein (**3**) hydrolysis.

point of the progress curve, the distribution of droplet fluorescence shows a well-defined single peak, indicating the presence of only a single population (Figure S2 available online). This result, together with the observation that the estimated number of compartmentalized cells equals the number of droplets exhibiting fluorescence (i.e., 2% of all droplets), establishes that single cells predominate in compartments and that cells are not aggregating. Access to single-cell measurements is enabled by the addition of silica nanoparticles (Percoll) that reduce cell sedimentation by density matching of the cell suspension, with the consequence that no cell aggregation is observed (Huebner et al., 2008; Shim et al., 2009).

A Workflow for Directed Evolution: Library Screening in Droplets

To carry out directed evolution cycles, the cell lysate assay described earlier was integrated with a sorting module. The individual steps of this workflow are shown in Figure 1, starting with protein expression (Step 1) and compartmentalization (Step 2), as described earlier. After the reaction was allowed to proceed in droplets in the collection syringe (Figure 1, Step 3), the droplets were reinjected into a second microfluidic device, a fluorescence-activated droplet sorter (Baret et al., 2009) for the assessment of the enzyme variants. Here, droplets above a chosen fluorescence threshold were separated dielectrophoretically (Figure 1, Step 4; Movie S1). These selected droplets were broken up, and their plasmid content was isolated to be electroporated into *E. coli* cells for starting the next evolution cycle.

To test whether this screening workflow (Figure 1) successfully delivers improved enzymes, PAS libraries were screened for increased promiscuous hydrolytic activity toward phosphonate **3**. An error-prone PCR library (Lib0) of PAS (8×10^5 transformants) was constructed by pooling a low mutational rate library with a higher mutational rate library, with averages of 1.5 and 3 mutations per gene, respectively. The combined library was screened as shown in Figure 1. In the first round of screening, 2×10^6 PAS-expressing cells (slightly exceeding the library size) were compartmentalized into 10^7 monodisperse droplets along with 250 μM phosphonate **3**. After collection in a syringe and incubation (1 hr), droplets were reinjected into the sorting chip to detect fluorescent product **1**. The brightest 4% of the cell-containing droplets (8×10^4 of 2×10^6 droplets) were separated at a frequency of 1 kHz. The plasmid DNA recovered from positive hits was purified and electroporated into *E. coli* for further rounds of sorting. Three rounds of sorting (resulting in library Lib1-Lib3) finally yielded an estimated library size of a hundred members. To achieve higher accuracy in the second

and third rounds of screening, the cell/droplet ratio was reduced (as the library size decreased) from 1:5 to 1:10 and 1:20, respectively. Decreasing the cell/droplet ratio gradually reduced the number of droplets with coencapsulated single cells. The extent of coencapsulation is dictated by the Poisson distribution (i.e., a function of the cell concentration) and partly determines the number of false-positives in dielectrophoretic droplet sorting (Baret et al., 2009). After the third round, 500 clones of the resulting library were rescreened in 96-well plates to isolate individual clones. The top 10% of the clones (with at least 4-fold improved activities) were sequenced and their activities quantified (Table S2). After purification, the best mutant, PAS^{A75G,R390C}, exhibited a 6-fold improvement in k_{cat}/K_M ($1.3 \times 10^4 \text{ M}^{-1} \text{ s}^{-1}$), validating its selection (Figure S3).

To quantitate the enrichment after each round of sorting, activity distributions of the libraries were measured in microtiter plates (Figure 4). Here, enrichment is considered as the frequency increase of clones in the library exceeding the threshold of the sorting experiment. For example, in library Lib2 the top 4% of the clones show two times faster rates in cell lysate as PAS^{WT}. After sorting, these clones represent 50% of the library Lib3, yielding an enrichment factor of 12.5 (50/4). The first two rounds of sorting gave slightly lower enrichments (9- and 4-fold, respectively), presumably because of a higher cell/droplet ratio that results in more co-compartmentalized cells. Over the three rounds, the cumulative enrichment factor is ~ 450 ($12.5 \times 4 \times 9$).

To demonstrate that the higher number of library members accessible in droplet experiments was crucial for the identification of improved enzyme variants, a moderately sized plate screening effort (4,000 clones) was carried out to screen PAS Lib0. This experiment showed no clones with significantly improved rates, giving a lower estimate for the frequency of clones having 2-fold increased activity as $<0.025\%$. This comparison gives an enrichment value for the three rounds of droplet screening as 2,000 (50/0.025). To further confirm this result, we also screened a smaller PAS library (Lib0') in droplets, consisting of only 2×10^4 variants. After three rounds of sorting, this library was also enriched and the best variants showed only 2-fold improved rates in cell lysates compared to PAS^{WT} (Figure S3). Taken together, these results suggest that clones with 6-fold improved activities are rare in Lib0 and imply that the increase in throughput afforded by droplet miniaturization was necessary to isolate these hits.

For the following round of evolution, eight of the selected sequences from Lib3 were pooled to generate a new error-prone PCR library of 8×10^5 variants. Since activities were significantly improved, the expression level was adjusted downward to remain in a convenient time window for screening. Protein expression levels were lowered by variation of isopropyl- β -D-thiogalactoside (IPTG) concentration and by introducing point mutations into the promoter region (see Experimental Procedures). This procedure is equivalent to the variation of enzyme concentration in conventional microtiter plate procedures by adjusting the quantity of cell lysate pipetted into the reaction assays. After three rounds of sorting improved variants were enriched and the best hits identified, showing up to 6-fold improved rates in lysates. Analysis of protein expression by SDS-PAGE gels indicated that the 6-fold improved observed rates were due to improved expression or solubility of the mutant enzymes (Figure S3).

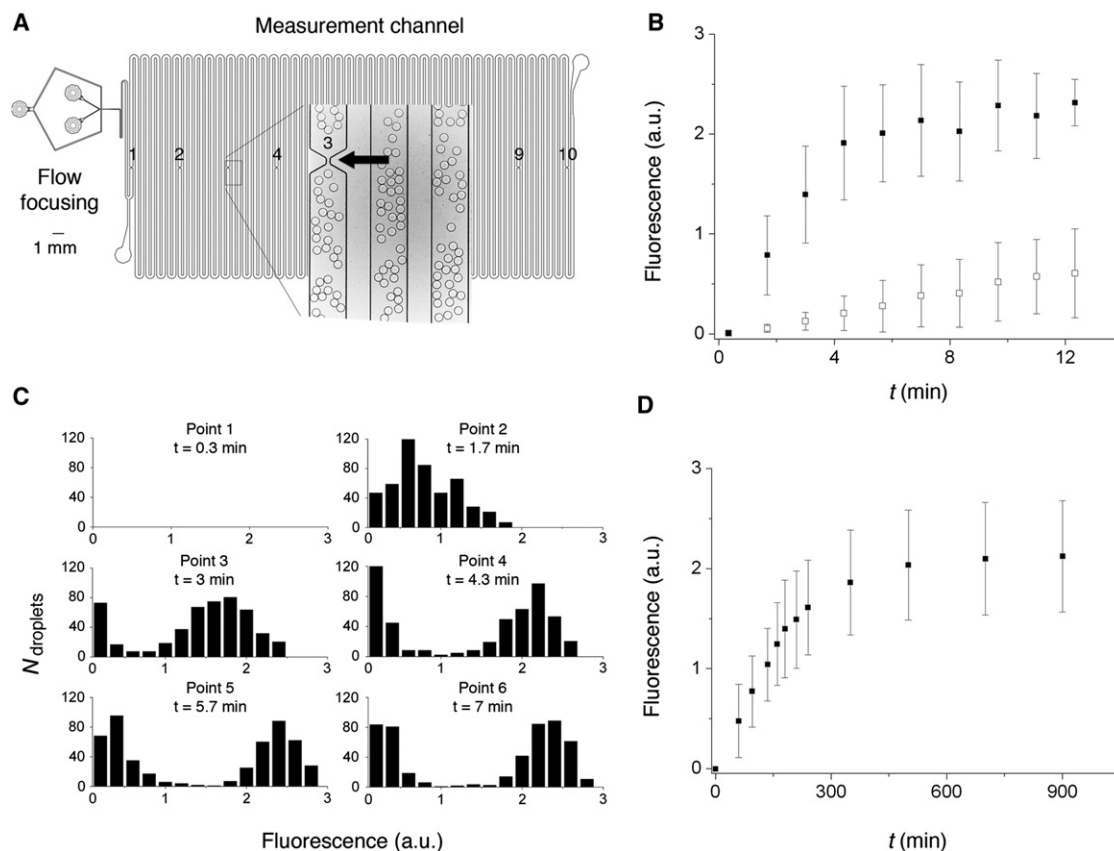


Figure 3. Time-Dependent Fluorescent Assays of Single Cell Lysates in Droplets

(A) The microfluidic delay line for on-chip measurement of reaction progress downstream of droplet formation (by retaining droplets for up to 12 min). The concentration of product **1** was assessed by laser-induced fluorescence detection at the 10 restriction points situated along the channel (the third measurement point is denoted by an arrow in the enlarged inset).

(B) The reaction of PAS^{WT} (■) and a slower variant PAS^{H46Y,M72V} (□) with sulfate **2** (25 μM). Each time point represents the mean fluorescence of 400 single cell-containing droplets (<3% of all droplets) and their SDs.

(C) The reaction of PAS^{WT}- and PAS^{H46Y,M72V}-expressing cells (1:1) with sulfate **2** (25 μM) represented in histograms to show the distribution of droplet populations, suggesting that a clear separation of active and less active clones is possible in the sorter (Figure 1).

See Figure S2A for a three-dimensional representation of the data (including all time points).

(D) The reaction of PAS^{WT} with phosphonate **3** (300 μM). To monitor reactions for longer periods, droplets were sampled into the measurement chip at different time points from an incubation syringe. The absence of leakage of the fluorophore is confirmed by the steady fluorescence level observed up to 16 hr.

See the Discussion and Table S1 for a comparison of the signal quality with other high-throughput screening methodologies.

Genotype Recovery from Droplets

For recovering the genotype of the selected clones from droplets, two experimental alternatives were tested, PCR and electroporation. We found that PCR is sensitive enough to recover even just a few DNA molecules, but undesired DNA recombination lowered the number of active clones in the sample after sorting, which compromised the hit rate. By contrast, direct transformation of the sorted sample into cells obviates the need for PCR amplification and cloning, thus preventing template recombination and the introduction of new mutations, as well as amplification bias (Williams et al., 2006). In addition, direct transformation is considerably faster.

To test the efficiency of DNA recovery from the sorted droplets by electroporation, low quantities of PAS-bearing plasmid DNA (pRSF-PAS) were electroporated and the numbers of transformed cells analyzed (Figure 5A). The measurements show that 1 in 400 plasmid copies leads to a transformant. Conse-

quently, a high copy number plasmid is necessary for efficient recovery. For pRSF-PAS, we measured 1,000 plasmid copies in one cell, which is reduced to 800 in the process of sample preparation for electroporation (for details, see Experimental Procedures). Thus, the plasmid content of a droplet containing a single cell is sufficient to transform two cells (800/400). This calculation is confirmed by the experimental observation that over the seven rounds of sorting, the number of transformed cells was twice the number of sorting events (Figure 5B).

The probability, P_i , that a particular sequence i is retransformed from the sorted sample can be estimated according to Equation 1 based on the assumption that every positive hit is sorted with equal likelihood (Bosley and Ostermeier, 2005):

$$P_i = 1 - \left(1 - \left(\frac{R}{N}\right)\right)^T, \quad (1)$$

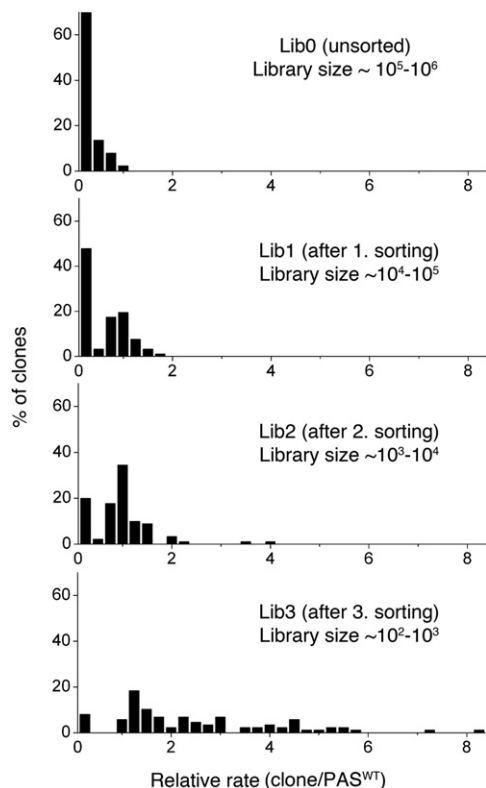


Figure 4. Enrichment of Positive Hits over Three Rounds of Droplet Sorting

Relative rates of 96 clones that were randomly picked from the original library (Lib0) and after each round of sorting (Lib1–Lib3). The data were normalized to the rate of PAS^{WT} . The frequency of positive hits in library Lib3 increased >2,000-fold compared to the starting library Lib0.

See Table S2 and Figure S3 for further data on the effects of the upcoming mutations and their positions.

where, R is the redundancy in the sorted sample, N is the number of sorting events, and T is the number of transformants obtained by the electroporation of the sorted sample. Since the experimental results show that $2N = T$, Equation 1 leads to the conclusion that 86.5% of the clones from the sorted sample ($P_i = 0.865$) are retransformed, if every positive clone is selected by sorting just once ($R = 1$). Thus, given that we oversampled the library during compartmentalization, we estimate that positive clones were recovered with 98% probability.

DISCUSSION

The utility of *in vitro* compartmentalization for directed evolution has been shown in several formats (Griffiths and Tawfik, 2006; Kintsos et al., 2010; Leemhuis et al., 2005). Here, the potential of droplet-based screening principles has been realized further by developing a workflow for cell lysate assays. Controlled cell lysis upon droplet formation in microfluidic channels makes it possible to perform high-throughput and high-fidelity assays. The reaction of PAS^{WT} with phosphonate **3** showed an average variation coefficient of the signal (SD/mean fluorescence) 0.3, in agreement with a previous study with microfluidic droplets

(Huebner et al., 2008). This variance is 3-fold lower compared to previous high-throughput activity-based screening methodologies (Table S1), e.g., bulk double emulsion format (Mastrobattista et al., 2005) or single-cell sorting (Aharoni et al., 2006; Varadarajan et al., 2005), and is only 2- to 3-fold worse than the corresponding value for the same reaction in 96-well plate format (0.15 or 0.09 after correction for variation introduced by the lysis procedure), despite the million-fold volume reduction (picoliter versus microliter assays). This slight increase in signal variation is necessarily due to expression variation at the single-cell level (Pedraza and van Oudenaarden, 2005). The gradual enrichment of library members with improvements in activity (6-fold) and expression (6-fold) validates that the workflow is suitable for the miniaturization of standard cell lysate experiments that are normally conducted on the microscale. The procedure enables the analysis of 10^7 droplets in 3 hr and the accomplishment of a whole screening cycle in 2 days, including cell growth and retransformation. In this way, the system is not only a million-fold more economical than microtiter plate screening but also two orders of magnitude faster than the maximum screening capacity of advanced robotic screening systems per day (10^5). These features will provide a unique advantage over traditional cell lysate assays, especially if expensive reagents are involved or for libraries where hit rates are low and improvements are small. For the all-too-common case of a deadlocked directed evolution campaign, rescue may come from the screening of a larger number of library members. Well-established selection schemes are applied routinely for the evolution of protein binders but are more difficult for enzymes where droplets have a unique role as a *screening* system for multiple-turnover catalysis at ultrahigh throughput. Other contemporary approaches to facilitate directed evolution (e.g., neutral drift, statistical prediction including consensus analysis, targeted mutagenesis of key residues, or the management of mutational load versus stability) (Gumulya and Reetz, 2012; Jäckel and Hilvert, 2010; Tokuriki and Tawfik, 2009; Tracewell and Arnold, 2009) are complementary to an increase in throughput and can be evaluated by insight into the precise fitness landscapes that the data from droplet experiments will yield.

This work extends a previous evolution experiment with yeast-displayed enzyme libraries in microfluidic droplets, where a droplet generation module was integrated with a droplet sorter via a short delay line. Using this setup, an already very efficient horseradish peroxidase activity (k_{cat}/K_M 10^7 $M^{-1}s^{-1}$) was improved by an order of magnitude (Agresti et al., 2010). Our workflow makes microfluidic droplet sorting accessible for proteins that are incompatible with yeast expression or cannot be displayed in their active form (such as PAS). Since cytoplasmic expression is the most robust route for protein production, cell lysate assays are among the most frequently used screening procedures. Protein production in *E. coli* results in high yields and is based on well-established procedures for genetic manipulation, rendering the workflow described here generally applicable. Slow and fast reactions become accessible in a flexible format, in which droplets are incubated off-chip and catalytic turnover is assessed on-chip (after a chosen incubation period). The adjustable expression further allows general variation of the level of product formation, and the control over these factors widens the dynamic range of starting activities that can be

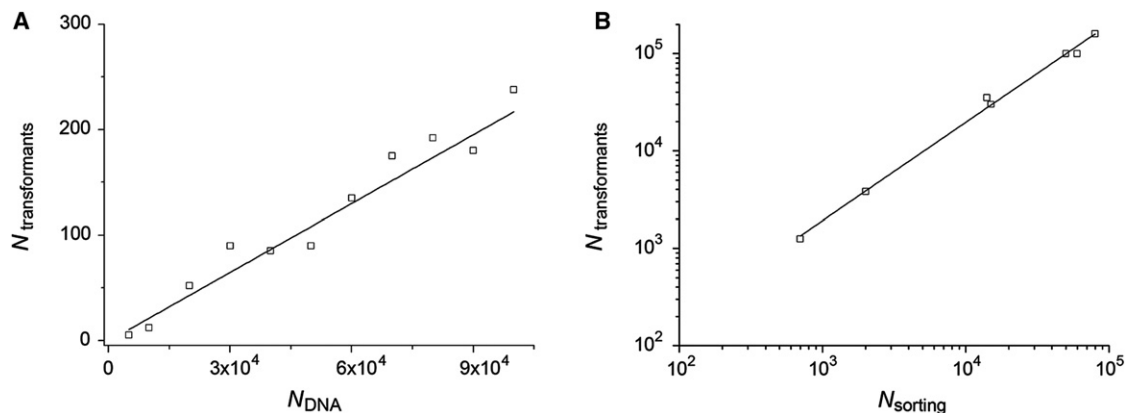


Figure 5. Elaboration of Electroporation Suitability for Efficient Recovery of Sorted Clones

(A) Efficiency of *E. coli* electroporation ($N_{DNA}/N_{transformants}$) with decreasing amount of PAS-pRSF plasmid DNA. The correlation is linear, and, even in the low concentration range, 400 plasmid molecules are enough to transform a single cell. Conditions: 25 μ l of *E. coli* cells (*E. coli* 10G Supreme, Lucigen), mixed with 1 μ l plasmid preparation in pure water, electroporation: 1,800 V, 1 mm gap cuvette).

(B) Correlation between the number of sorting events ($N_{sorting}$) and the number of recovered clones ($N_{transformants}$) over seven rounds of screening using the fluorescent-activated droplet sorter.

gradually improved in the course of an evolution experiment. The dynamic range can still be extended downward by longer incubation times (to allow more time for reaction), which may require improved retention of fluorophores by substrate manipulation (Woronoff et al., 2011) or altered emulsion formulations (Courtois et al., 2009). Alternatively, increased enzyme levels can be brought about by letting a compartmentalized cell proliferate prior to the enzymatic assay, so that enzymes with very low catalytic efficiency (k_{cat}/K_M lower than $10 \text{ M}^{-1}\text{s}^{-1}$) may become accessible for evolution. Screening in droplet formats is currently dependent on assays that generate a fluorescent reaction product, but other optical readouts, including absorbance (Deal and Easley, 2012) or Raman detection (Cecchini et al., 2011), may become available in the future. This versatility together with high-throughput and the ability to carry out precise yet miniaturized assays will prove useful for a variety of applications in directed evolution, but also for exploring metagenomic and genomic library diversity, to improve and identify enzymes with new catalytic activities.

SIGNIFICANCE

Directed evolution relies on efficient technologies to explore sequence space. Monoclonal microdroplets that compartmentalize genotype and phenotype in water-in-oil emulsions provide a unique screening format in which catalytic turnover can be measured directly to provide kinetic data on every library member. The potential to investigate larger numbers of droplets generated in microfluidic chips ($3.6 \times 10^6/\text{hr}$) is accompanied by an assay quality that is similar to microplate screening systems, despite the million-fold reduction in volume. The availability of a validated, straightforward, and sensitive screening procedure that allows efficient recovery of hits with even subtle improvements, and is not encumbered by potential reduction of diversity by PCR amplification steps, brings this new technology closer to a wider application. In the future, the ability to characterize

each member of an entire library may allow the manipulation of directed evolution experiments in a more strategic way, based on measurement of “fitness landscapes” of proteins. The flexibility of setting thresholds and varying selection criteria will thus enable directed evolution in a highly controlled way.

EXPERIMENTAL PROCEDURES

Arylsulfatase Libraries and Manipulation of Expression Levels

PAS was randomly mutated by error-prone PCR (epPCR), using mutazyme II low-fidelity polymerase (Stratagene) with an average of 1.5 and 3 mutations per gene. The two PCR products were ligated into a modified pRSFDuet vector (Novagene) and were combined in a ratio of 1:10, together giving an estimated library size of 8×10^5 . This library provides near-certain coverage for all single- and double-amino-acid mutants that are available by error-prone PCR. The same library creation strategy was followed in the second round of evolution and with Lib0'. The following T7 promoter variants with lower expression level were produced in the modified pRSFDuet vector: (1) mutation at position -7 from C to G (reduced expression by 20-fold); (2) mutation at position -9 from C to G (reduced by 50-fold); and (3) the combination of mutations at position -5 from C to A, at -7 from C to G, and at -9 from C to G (reduced by 100-fold). The expression levels were determined by measuring the activity of PAS^{WT} in microtiter plate cell lysate assay. Note that comparison of the measured expression levels to a previous study (Ikeda et al., 1992) suggested that the effects of the mutations strongly depend on the copy number of the plasmid. We found that the T7 promoter can be regulated by varying the IPTG concentration, possibly as a result of the very high copy number of the plasmid pRSFDuet in *E. coli* BL21 (DE3).

Preparation of Cells for Compartmentalization

E. coli BL21 (DE3) cells were transformed with plasmid library pRSF-PAS, and expression was carried out in 10 ml cell cultures overnight as described (Huebner et al., 2008). A 1 ml aliquot of the cell culture was washed (100 mM MOPS, 100 mM NaCl, pH 8.0) and filtered with a 5 μ m syringe filter (Sartorius), and its absorbance was recorded at 600 nm. Then, cells were diluted in the same buffer containing 25% Percoll (silica nanoparticles preventing cell-cell adhesion and increasing density of the buffer to prevent cell sedimentation during the experiments; Sigma-Aldrich) For a droplet diameter of 35 μ m, values for $A^{600\text{nm}}$ of 0.15 and 0.02 resulted in 20% and 3% occupancy, respectively. All solutions (except for cell suspensions) were filtered before compartmentalization with 0.45 μ m syringe filters (Sartorius) to avoid the clogging of microfluidic channels.

Microfluidic Device Fabrication

Poly(dimethyl)siloxane (PDMS) devices were fabricated using standard soft lithographic procedures largely as described elsewhere (Huebner et al., 2008). The following alterations to the procedure were made: the photoresist material SU-8 2025 (MicroChem) was spin-coated on the silicon wafer at 500 rpm for 5 s and ramped to 1,000 rpm at an acceleration of 300 rpm/s for 30 s. In this way, the final thickness to the film layer was increased, giving a channel height of 25 μm in the device. After sealing the PDMS device to a microscope slide, the surface of the channels was modified with Trichloro(1H,1H,2H,2H-perfluorooctyl)silane (Sigma) in fluorinated oil HFE-7500 (1%, w/w; 3M) to avoid wetting of the droplets on the channel walls. In the case of the sorting device, an extra PDMS layer was integrated between the channel and the microscope slide in order to separate the electrodes from the glass slide, avoiding electrical shortcuts (Figure S1). The channels built for the electrodes in the sorting device (Figure S1) were filled with low-melting-point indium composite solder (51 In/32.5 Bi/16.5 Sn; Indium Corporation) after the device was heated on a hot plate (145°C). Copper wire (length, 2 cm) was introduced into the molten metal through the entrance holes of the channels, serving as electrical contacts (Figure S1).

Flow-Focusing Device Operation

Droplet formation was carried out using the flow-focusing device shown in Figure 1 and Figure S1. The nozzle size was 20 μm , and the channel height was 25 μm . The device featured two aqueous streams: one containing the cell solution, and the other containing the substrate and cell-lysing agents BugBuster (35%, w/w; Merck) and rLysozyme (0.4%, w/w; Novagen) in a buffer 100 mM MOPS, 100 mM NaCl, pH 8.0. Note that concentrations are given prior to mixing. Higher detergent concentrations were found to perturb droplet formation. For flow control, plastic syringes (1 ml, Norm-Ject) or SGE glass syringes (100 μl , for flow rates lower than 20 $\mu\text{l/hr}$) were driven by syringe infusion pumps (Harvard Apparatus 2000) and connected to the device by polyethylene tubing (inner diameter, 0.38 mm; Intramedic). The oil phase consisted of a fluorinated oil HFE-7500 (3M) with EA surfactant (0.7%, w/w; Raindance). Droplet formation was monitored through a 10 \times microscope objective (UPlanFLN, Olympus) by a Phantom V72 fast camera mounted on the microscope (IX71, Olympus).

Kinetic Measurements in Droplets and Optical Set-Up

Short kinetic measurements (up to 12 min) were carried out in a delay line built in after the flow-focusing device (Figure 3A). To generate droplets with a diameter 30–40 μm , the aqueous streams were driven at a rate 10 $\mu\text{l/hr}$ and the oil phase was 120 $\mu\text{l/hr}$. The fluorescence of the moving droplets were measured at restriction points 20 μm wide situated along the delay line, where a laser beam (Picarro Cyan solid state laser; 20 mW, 488 nm) was focused through a 40 \times microscope objective (UPlanFLN mounted). Detection was carried out through the same objective by a photomultiplier tube (H8249, Hamamatsu Photonics). To remove the 488 nm excitation light, the fluorescent light was transmitted through a dichroic beam splitter (FF409-Di02, Semrock) in the microscope filter box. Another dichroic (FF555-Di02, Semrock) built before the photomultiplier tube was used to split up the green fluorescence and a red illumination (Figure S1), which was used to record pictures using a fast camera (Phantom V72). A band-pass filter (516–530 nm) placed on the photomultiplier was used to remove residual red light going into the detector. At each time point, the fluorescence value represents the average fluorescence of 400 droplets, which was recorded on to a data acquisition card (National Instruments), and analyzed using a peak detection algorithm in LabView 8.2 (National Instruments). For longer recordings, droplets were stored off-chip in a 1 ml plastic syringe (Norm Ject) and reinjected into the microfluidic channel for measurements at desired time points. The plastic syringe for droplet collection was connected to the polyethylene tubing without using a hydrophilic metal needle that would have decreased the stability of the droplets. The syringe was also filled with 100 μl of oil prior to droplet collection.

Calibration curves suggest that a minimum fluorescein concentration of 10–100 nM can be readily detected with this optical set-up. The sensitivity limit for catalytic turnover depends on the signal change before and after reaction (i.e., the fluorescence change between substrate and product and effects from possible product contamination of the starting material), the substrate concentration, and the noise in the measurements. In our case, complete hydrolysis of the substrates bis(methylphosphonyl)fluorescein and fluorescein disulfate

gives a 100-fold fluorescence increase. A 2-fold signal change can reliably be detected in droplet-based assays, so the minimum product concentration that can be detected is the turnover of 1%–2% of the substrate.

Sorting Experiments

The flow-focusing device was used to generate droplets for sorting, with flow rates for the aqueous and the oil phases set to 200 $\mu\text{l/hr}$ and 1,300 $\mu\text{l/hr}$, respectively. This set-up resulted in the formation of droplets 35 μm in diameter, at a rate of 6 kHz. After droplet formation stabilized (\sim 3 min), a plastic syringe was connected to the device outlet for the collection of the droplets. After 1 hour of incubation, droplets were reinjected into a sorting device (Figure 1; Figure S1) that was modeled on a previous design (Baret et al., 2009). To avoid sorting of multiple droplets with a single electric pulse, the distance between droplets was increased by introducing extra oil into the channel at a rate of 2 \times 400 $\mu\text{l/hr}$. When droplets are injected at a rate of 60 $\mu\text{l/hr}$, this set-up results in a sorting rate of \sim 1 kHz. The asymmetric Y-shape of the sorting junction ensures that droplets flow automatically into the wider waste channel, having a lower flow resistance. The relative resistance of the waste and the collection channels was further adjusted by back-pressure controllers (electrical connector strips) equipped on to the connected polyethylene tubing at the outlets. The laser beam was focused 50 μm upstream of the sorting junction through the 40 \times microscope objective (UPlanFLN, Olympus). The photomultiplier was connected to a pulse generator (TGP110, Thurlby Thandar Instruments) that triggered a square pulse (0.5–1 ms) when the fluorescence signal reached a threshold. This pulse was amplified 1,000-fold to 0.6–0.8 kV by a high voltage amplifier (610E, Trek) and applied to the electrodes in the sorting device. To drive the selected droplets into the collection channel, the required pulse settings may be varied (e.g., length or amplitude), depending on droplet frequency, flow rates, and droplet size: the bigger the droplets and the higher the flow rates, the more stronger pulses are needed. However, the higher flow rates also required shorter pulses to ensure that only single droplets were selected. The settings were adjusted before each sorting experiment to achieve optimal performance, which was verified by using the recordings of the fast camera. Being lighter than the fluorinated oil carrier phase, the sorted droplets accumulate in the top part of a bent tube connected to the device outlet (Figure S1C) and can be conveniently harvested despite their small volume (\sim 20 pl \times 10⁵ correspond to 2 μl).

DNA Recovery from Droplets by Transformation and Determination of Its Efficiency

After sorting, droplets were transferred from the polyethylene collection tubing (Figure S1) into an Eppendorf tube that had been pre-filled with 50 μl water (Millipore Synergy). Droplets spontaneously assemble at the water-oil interface, where their contents were released into the aqueous phase by the addition of 100 μl 1H,1H,2H,2H-perfluorooctanol in HFE-7500 oil (50%, w/w). Then the aqueous phase was decanted and purified on a spin column (DNA Clean & Concentrator-5, Zymo Research). Plasmid DNA was eluted in 10 μl pure water and transformed into 4 \times 25 μl electrocompetent *E. coli* cells (*E. coli* 10G Supreme, Lucigen). For the determination of electroporation efficiency, purified PAS-pRSFDuet plasmid miniprep was diluted in pure water to defined concentrations, and these samples were electroporated into *E. coli* 10G Supreme cells (Lucigen). Electroporation efficiency was calculated as $N_{\text{plasmid DNA}}/N_{\text{transformed cells}}$. Note that the electroporation efficiency strongly depends on the size of the plasmid; thus, significantly bigger plasmids may give insufficient electroporation efficiency. The copy number of PAS-pRSFDuet (5,800 base pairs) in *E. coli* BL21 (DE3) cells was determined using the cell cultures that were applied for compartmentalization. One-milliliter cell suspension of $A^{600\text{nm}} = 1$ was used to purify PAS-pRSFDuet by a standard spin column DNA miniprep kit (QIAGEN). The DNA yield (\sim 1 μg) was measured in a NanoDrop 2000c spectrophotometer (Thermo Scientific) and correlated to the number of cells in the culture that was counted as 2×10^8 cell/ml when $A^{600\text{nm}}$ was 1. The loss of DNA during purification was determined as 20%.

Synthesis of Bis(methylphosphonyl)fluorescein and Bis(sulfate)fluorescein

The synthesis of bis(methylphosphonyl)fluorescein and bis(sulfate)fluorescein was performed as described for fluorescein phosphates and sulfates (Scheitz et al., 1997). The detailed procedure and the characterization of bis

(methylphosphonyl)fluorescein are included into the [Supplemental Experimental Procedures](#).

SUPPLEMENTAL INFORMATION

Supplemental Information includes three figures, two tables, one movie, and Supplemental Experimental Procedures and can be found with this article online at <http://dx.doi.org/10.1016/j.chembiol.2012.06.009>.

ACKNOWLEDGMENTS

This research was funded by a Research Councils UK Basic Technology Grant, the European Union (EU) New and Emerging Science and Technology Project MiFem, and the Biotechnology and Biological Sciences Research Council. B.K., F.C., and M.F. held fellowships from the EU Marie-Curie Programme, and M.F.M. holds a fellowship from the Natural Sciences and Engineering Research Council of Canada. F.H. is a European Research Council Starting Investigator. The authors thank Graeme Whyte and the Microdroplets Group at the University of Cambridge for technical advice, Nobuhiko Tokuriki for helpful discussions, Pietro Gatti-Lafranconi for a critical reading of the manuscript, and the reviewers for their detailed criticism and suggestions.

Received: April 6, 2012

Revised: May 31, 2012

Accepted: June 4, 2012

Published: August 23, 2012

REFERENCES

- Agresti, J.J., Antipov, E., Abate, A.R., Ahn, K., Rowat, A.C., Baret, J.C., Marquez, M., Klibanov, A.M., Griffiths, A.D., and Weitz, D.A. (2010). Ultrahigh-throughput screening in drop-based microfluidics for directed evolution. *Proc. Natl. Acad. Sci. USA* *107*, 4004–4009.
- Aharoni, A., Amitai, G., Bernath, K., Magdassi, S., and Tawfik, D.S. (2005). High-throughput screening of enzyme libraries: thiolactonases evolved by fluorescence-activated sorting of single cells in emulsion compartments. *Chem. Biol.* *12*, 1281–1289.
- Aharoni, A., Thieme, K., Chiu, C.P., Buchini, S., Lairson, L.L., Chen, H., Strynadka, N.C., Wakarchuk, W.W., and Withers, S.G. (2006). High-throughput screening methodology for the directed evolution of glycosyltransferases. *Nat. Methods* *3*, 609–614.
- Babtie, A., Tokuriki, N., and Hoffelder, F. (2010). What makes an enzyme promiscuous? *Curr. Opin. Chem. Biol.* *14*, 200–207.
- Babtie, A.C., Bandyopadhyay, S., Olguin, L.F., and Hoffelder, F. (2009). Efficient catalytic promiscuity for chemically distinct reactions. *Angew. Chem. Int. Ed. Engl.* *48*, 3692–3694.
- Baret, J.C., Miller, O.J., Taly, V., Ryckelynck, M., El-Harrak, A., Frenz, L., Rick, C., Samuels, M.L., Hutchison, J.B., Agresti, J.J., et al. (2009). Fluorescence-activated droplet sorting (FADS): efficient microfluidic cell sorting based on enzymatic activity. *Lab Chip* *9*, 1850–1858.
- Bertschinger, J., Grabulovski, D., and Neri, D. (2007). Selection of single domain binding proteins by covalent DNA display. *Protein Eng. Des. Sel.* *20*, 57–68.
- Boltes, I., Czapińska, H., Kahnert, A., von Bülow, R., Dierks, T., Schmidt, B., von Figura, K., Kertesz, M.A., and Usón, I. (2001). 1.3 Å structure of arylsulfatase from *Pseudomonas aeruginosa* establishes the catalytic mechanism of sulfate ester cleavage in the sulfatase family. *Structure* *9*, 483–491.
- Bornscheuer, U.T., and Kazlauskas, R.J. (2004). Catalytic promiscuity in biocatalysis: using old enzymes to form new bonds and follow new pathways. *Angew. Chem. Int. Ed. Engl.* *43*, 6032–6040.
- Bosley, A.D., and Ostermeier, M. (2005). Mathematical expressions useful in the construction, description and evaluation of protein libraries. *Biomol. Eng.* *22*, 57–61.
- Cecchini, M.P., Hong, J., Lim, C., Choo, J., Albrecht, T., Demello, A.J., and Edel, J.B. (2011). Ultrafast surface enhanced resonance Raman scattering detection in droplet-based microfluidic systems. *Anal. Chem.* *83*, 3076–3081.
- Courtois, F., Olguin, L.F., Whyte, G., Bratton, D., Huck, W.T., Abell, C., and Hoffelder, F. (2008). An integrated device for monitoring time-dependent in vitro expression from single genes in picolitre droplets. *ChemBioChem* *9*, 439–446.
- Courtois, F., Olguin, L.F., Whyte, G., Theberge, A.B., Huck, W.T., Hoffelder, F., and Abell, C. (2009). Controlling the retention of small molecules in emulsion microdroplets for use in cell-based assays. *Anal. Chem.* *81*, 3008–3016.
- d'Abbadie, M., Hofreiter, M., Vaisman, A., Loakes, D., Gasparutto, D., Cadet, J., Woodgate, R., Pääbo, S., and Holliger, P. (2007). Molecular breeding of polymerases for amplification of ancient DNA. *Nat. Biotechnol.* *25*, 939–943.
- Deal, K.S., and Easley, C.J. (2012). Self-regulated, droplet-based sample chopper for microfluidic absorbance detection. *Anal. Chem.* *84*, 1510–1516.
- Fallah-Araghi, A., Baret, J.C., Ryckelynck, M., and Griffiths, A.D. (2012). A completely in vitro ultrahigh-throughput droplet-based microfluidic screening system for protein engineering and directed evolution. *Lab Chip* *12*, 882–891.
- Frenz, L., Blank, K., Brouzes, E., and Griffiths, A.D. (2009). Reliable microfluidic on-chip incubation of droplets in delay-lines. *Lab Chip* *9*, 1344–1348.
- Griffiths, A.D., and Tawfik, D.S. (2006). Miniaturising the laboratory in emulsion droplets. *Trends Biotechnol.* *24*, 395–402.
- Gumulya, Y., and Reetz, M.T. (2012). Many pathways in laboratory evolution can lead to improved enzymes: how to escape from local minima. *ChemBioChem* *13*, 1060–1066.
- Gupta, R.D., Goldsmith, M., Ashani, Y., Simo, Y., Mullokandov, G., Bar, H., Ben-David, M., Leader, H., Margalit, R., Silman, I., et al. (2011). Directed evolution of hydrolases for prevention of G-type nerve agent intoxication. *Nat. Chem. Biol.* *7*, 120–125.
- Huebner, A., Srisa-Art, M., Holt, D., Abell, C., Hoffelder, F., deMello, A.J., and Edel, J.B. (2007). Quantitative detection of protein expression in single cells using droplet microfluidics. *Chem. Commun. (Camb.)* (12), 1218–1220.
- Huebner, A., Olguin, L.F., Bratton, D., Whyte, G., Huck, W.T., de Mello, A.J., Edel, J.B., Abell, C., and Hoffelder, F. (2008). Development of quantitative cell-based enzyme assays in microdroplets. *Anal. Chem.* *80*, 3890–3896.
- Ikeda, R.A., Warshamana, G.S., and Chang, L.L. (1992). In vivo and in vitro activities of point mutants of the bacteriophage T7 RNA polymerase promoter. *Biochemistry* *31*, 9073–9080.
- Jäckel, C., and Hilvert, D. (2010). Biocatalysts by evolution. *Curr. Opin. Biotechnol.* *21*, 753–759.
- Jonas, S., and Hoffelder, F. (2009). Mapping catalytic promiscuity in the alkaline phosphatase superfamily. *Pure Appl. Chem.* *81*, 731–742.
- Khersonsky, O., and Tawfik, D.S. (2010). Enzyme promiscuity: a mechanistic and evolutionary perspective. *Annu. Rev. Biochem.* *79*, 471–505.
- Kintses, B., van Vliet, L.D., Devenish, S.R., and Hoffelder, F. (2010). Microfluidic droplets: new integrated workflows for biological experiments. *Curr. Opin. Chem. Biol.* *14*, 548–555.
- Köster, S., Angilè, F.E., Duan, H., Agresti, J.J., Wintner, A., Schmitz, C., Rowat, A.C., Merten, C.A., Pisignano, D., Griffiths, A.D., and Weitz, D.A. (2008). Drop-based microfluidic devices for encapsulation of single cells. *Lab Chip* *8*, 1110–1115.
- Leemhuis, H., Stein, V., Griffiths, A.D., and Hoffelder, F. (2005). New genotype-phenotype linkages for directed evolution of functional proteins. *Curr. Opin. Struct. Biol.* *15*, 472–478.
- Lin, H., and Cornish, V.W. (2002). Screening and selection methods for large-scale analysis of protein function. *Angew. Chem. Int. Ed. Engl.* *41*, 4402–4425.
- Loakes, D., Gallego, J., Pinheiro, V.B., Kool, E.T., and Holliger, P. (2009). Evolving a polymerase for hydrophobic base analogues. *J. Am. Chem. Soc.* *131*, 14827–14837.
- Mastrobattista, E., Taly, V., Chanudet, E., Treacy, P., Kelly, B.T., and Griffiths, A.D. (2005). High-throughput screening of enzyme libraries: in vitro evolution of a beta-galactosidase by fluorescence-activated sorting of double emulsions. *Chem. Biol.* *12*, 1291–1300.
- Mazutis, L., Araghi, A.F., Miller, O.J., Baret, J.C., Frenz, L., Janoshazi, A., Taly, V., Miller, B.J., Hutchison, J.B., Link, D., et al. (2009). Droplet-based

- microfluidic systems for high-throughput single DNA molecule isothermal amplification and analysis. *Anal. Chem.* **81**, 4813–4821.
- Mohamed, M.F., and Hollfelder, F. (2012). Efficient, crosswise catalytic promiscuity among enzymes that catalyze phosphoryl transfer. *Biochim. Biophys. Acta*. <http://dx.doi.org/10.1016/j.bbapap.2012.07.015>.
- Niu, X., Gulati, S., Edel, J.B., and deMello, A.J. (2008). Pillar-induced droplet merging in microfluidic circuits. *Lab Chip* **8**, 1837–1841.
- O'Brien, P.J., and Herschlag, D. (1999). Catalytic promiscuity and the evolution of new enzymatic activities. *Chem. Biol.* **6**, R91–R105.
- Olguin, L.F., Askew, S.E., O'Donoghue, A.C., and Hollfelder, F. (2008). Efficient catalytic promiscuity in an enzyme superfamily: an arylsulfatase shows a rate acceleration of 10(13) for phosphate monoester hydrolysis. *J. Am. Chem. Soc.* **130**, 16547–16555.
- Pedraza, J.M., and van Oudenaarden, A. (2005). Noise propagation in gene networks. *Science* **307**, 1965–1969.
- Romero, P.A., and Arnold, F.H. (2009). Exploring protein fitness landscapes by directed evolution. *Nat. Rev. Mol. Cell Biol.* **10**, 866–876.
- Schaerli, Y., and Hollfelder, F. (2009). The potential of microfluidic water-in-oil droplets in experimental biology. *Mol. Biosyst.* **5**, 1392–1404.
- Scheigetz, J., Gilbert, M., and Zamboni, R. (1997). Synthesis of fluorescein phosphates and sulfates. *Org. Prep. Proced. Int.* **29**, 561–568.
- Shim, J.U., Olguin, L.F., Whyte, G., Scott, D., Babbie, A., Abell, C., Huck, W.T., and Hollfelder, F. (2009). Simultaneous determination of gene expression and enzymatic activity in individual bacterial cells in microdroplet compartments. *J. Am. Chem. Soc.* **131**, 15251–15256.
- Tawfik, D.S., and Griffiths, A.D. (1998). Man-made cell-like compartments for molecular evolution. *Nat. Biotechnol.* **16**, 652–656.
- Theberge, A.B., Courtois, F., Schaerli, Y., Fischlechner, M., Abell, C., Hollfelder, F., and Huck, W.T. (2010). Microdroplets in microfluidics: an evolving platform for discoveries in chemistry and biology. *Angew. Chem. Int. Ed. Engl.* **49**, 5846–5868.
- Tokuriki, N., and Tawfik, D.S. (2009). Stability effects of mutations and protein evolvability. *Curr. Opin. Struct. Biol.* **19**, 596–604.
- Tracewell, C.A., and Arnold, F.H. (2009). Directed enzyme evolution: climbing fitness peaks one amino acid at a time. *Curr. Opin. Chem. Biol.* **13**, 3–9.
- Turner, N.J. (2009). Directed evolution drives the next generation of biocatalysts. *Nat. Chem. Biol.* **5**, 567–573.
- Varadarajan, N., Gam, J., Olsen, M.J., Georgiou, G., and Iverson, B.L. (2005). Engineering of protease variants exhibiting high catalytic activity and exquisite substrate selectivity. *Proc. Natl. Acad. Sci. USA* **102**, 6855–6860.
- Williams, R., Peisajovich, S.G., Miller, O.J., Magdassi, S., Tawfik, D.S., and Griffiths, A.D. (2006). Amplification of complex gene libraries by emulsion PCR. *Nat. Methods* **3**, 545–550.
- Woronoff, G., El Harrak, A., Mayot, E., Schicke, O., Miller, O.J., Soumillon, P., Griffiths, A.D., and Ryckelynck, M. (2011). New generation of amino coumarin methyl sulfonate-based fluorogenic substrates for amidase assays in droplet-based microfluidic applications. *Anal. Chem.* **83**, 2852–2857.
- Yang, G., and Withers, S.G. (2009). Ultrahigh-throughput FACS-based screening for directed enzyme evolution. *ChemBioChem* **10**, 2704–2715.